Supporting Information

Enhanced Rigidification within a Double Mutant of Soybean Lipoxygenase Provides Experimental Support for Vibronically Nonadiabatic Proton-Coupled Electron Transfer Models

Shenshen Hu, [†§] Alexander V. Soudackov,[#] Sharon Hammes-Schiffer,[#] and Judith P. Klinman[†‡§*]

† Department of Chemistry, University of California, Berkeley, California 94720, United States

‡ Department of Molecular and Cell Biology, University of California, Berkeley, California 94720, United States

§ California Institute for Quantitative Biosciences, University of California, Berkeley, California 94720, United States

Department of Chemistry, University of Illinois at Urbana-Champaign, Urbana, Illinois, 61801, United States

*To whom correspondence should be addressed: klinman@berkeley.edu

Contents

I. Materials and Methods

1.1 General Information. All reagents were purchased from commercial sources and used without further purification unless otherwise indicated. Linoleic acid (>99% purity) (H-LA) was purchased from Sigma-Aldrich and purified again before usage. 11,11-$^{2}H_2$-Linoleic Acid (d_2-LA) and 13-(*S*)-HPOD were synthesized and purified according to the previous report.[1, 2]

1.2 Protein expression/purification. Double mutant L546A/L754A was prepared, expressed and purified according to the previous report,[3] with minor modification on the lysis method. The sonication lysis protocol was used in the current research, instead of BugBuster: Cell paste from 4.5 L (~30 g) was resuspended in ca. 75 mL lysis buffer (pH 7.5, 50 mM NaCl, 50mM NaPi, 10% glycerol, 0.1% Tween-20, 15 U/mL Benzonase, 0.25 KU/ml rLysozyme, 1 mM AEBSF). The lysis solution was stirred for 20 min at room temperature and sonicated for three cycles.

1.3 Kinetics Determination. Steady-state kinetics with protio-LA were performed on a Cary50 spectrophotometer in a single wavelength mode while discontinuous HPLC assays were used for the reaction of d_2-LA, as previously described.[3]

The K_m value of d_2-LA is estimated to be around 2 μM according to the $^{D}(k_{cat}/K_m)$ value (ca. ~30).[2] Thus, the reaction rate at a substrate concentration of 35 μM could be considered the maximum rate achieved at the saturating substrate concentration. The reaction rate under saturating substrate concentration was calculated using the standard curve of peak intensity vs HPOD concentration (Figure S4), which is further corrected for the concentrations of enzyme used in the separate assays to obtain $k_{cat\text{-}D}$.

UV and HPLC kinetics were performed under ambient atmosphere (>>20.8% O2). To convert the estimates of k_{cat} computed from UV kinetic data to values at saturating O_2, initial rate data were collected for a matrix of six O_2 concentrations that typically spanned from about 1% of ambient to pure O_2 and 35 μM H-LA concentrations. The rate of linoleic acid oxidation by the double mutants was monitored by oxygen consumption using a Clark-type electrode from Yellow Springs Inc. A 990-μl volume of buffer (0.1 M borate at pH 9) and LA was equilibrated to the desired temperature in a thermally controlled water-jacketed cell. Oxygen concentration was attained by maintaining a desired O_2/N_2 mixture in the head space above the substrate solution for 5 min. The reaction was initiated by the injection of a similarly buffered solution of lipoxygenase mutant. The $K_M(O_2)$ value for double mutant is too low to be measured (≤1 μM) at 10°C and 30°C. Thus, there was no need for the oxygen concentration correction.

1.4 Enzyme stability for discontinuous HPLC assays. As shown in Figure S5, kinetic traces with d_2-LA indicate a very long lag phase when assayed with DM-SLO: from around 3 hrs at 30°C that increases to 16 hrs when the temperature was decreased to 5°C. The previous study demonstrated that the addition of 1 eq. of 13-(*S*)-HPOD to oxidize the active Fe(II) to Fe(III) did not eliminate the lag phase at 30°C and, contrary to expectations, led to a loss of enzyme activity.[3] For the present study, no effort was made to preoxidize the active site metal, and controls were conducted to test for any time-dependent inactivation of DM-SLO during the long lag phases between 5 and 30° on the basis of the previous study.[3] In all cases, full maintenance of enzyme activity was observed in the experimental temperature range (Figure S6A-S6C). As shown in

Figure S6, the DM still maintained full activity at temperatures 5°C, 20°C and 30°C when incubating with d_2-LA for 16h, 5h, and 3.5 h, respectively (Figure S6A-S6C). Because of the observation that the DM-SLO loses 50% of its activity in the first one hour of incubation at 35°C (Figure S6D), no effort was made to collect detailed kinetic measurements above 30°C. While these properties lead to a more narrow temperature range for the collection of kinetic data than was possible in earlier studies of the WT SLO and the majority of its single site mutants,[1,4] it was still possible to assess trends in the temperature dependence of the KIEs, albeit with greater error bars.

1.5 Steady-state kinetics under high pressure.[5] Steady-state kinetics experiments of DM under pressures of 1, 344, 688 and 1034 bar were performed on a Cary 50 UV-visible spectrophotometer using a high-pressure cell (ISS, Champaign IL). The temperature was controlled with a water bath circulator at 15°C, 20°C, 25°C, 30°C and 35°C. Hydrostatic pressure was generated with a hand pump (High Pressure Equipment Company, Erie, PA) connected to the high-pressure cell by flexible tubing. De-ionized water was utilized as the pressure medium. A round quartz cuvette with a Teflon cork was used for the kinetic assays. The kinetic assays and protein stability assay under pressure were performed as previously described. Even with the deletions of two side chains, the protein stability assays showed that the double mutant still retained the ambient pressure activity following the reaction at 1,034 bar for 5 min, providing a time window for reliable kinetic measurements (Fig S7).

1.6 Nonadiabatic Fitting for WT and DM SLO.

The fitting of the temperature dependence of the experimentally measured KIE for the hydrogen tunneling in WT and DM-WT was performed using the nonadiabatic tunneling model described in Refs. 6, 7. Under the assumption of a harmonic DAD sampling mode characterized by the mass M, frequency Ω, and equilibrium DAD value R_0, the nonadiabatic rate constant is given by the following expression:

$$k = \frac{V^2}{\hbar}\sum_{\mu} P_{\mu}\sum_{\nu} S_{\mu\nu}^2 \exp\left[\frac{2\lambda_{\mu\nu}^{(\alpha)}\zeta}{\hbar\Omega + 2\lambda_{\mu\nu}^{(\gamma)}\zeta}\right]\left(1+\frac{2\lambda_{\mu\nu}^{(\gamma)}\zeta}{\hbar\Omega}\right)^{-\frac{1}{2}}\sqrt{\frac{\pi\beta}{\lambda}}\exp\left[-\frac{\beta\left(\Delta G_{\mu\nu}+\lambda_{\text{tot}}\right)^2}{4\lambda}\right] \quad \text{(S1)}$$

where the summations are over reactant and product electron-proton vibronic states (3 reactant and 3 product vibronic states were included), P_{μ} is the Boltzmann population of reactant state μ, λ_{tot} is the total reorganization energy, $\Delta G_{\mu\nu}$ is the reaction free energy for vibronic states μ and ν, $S_{\mu\nu}$ is the overlap integral between the hydrogen vibrational wavefunctions for states μ and ν at R_0, and V is the electronic coupling. Moreover, $\lambda_{\mu\nu}^{(\alpha)} = \hbar^2\alpha_{\mu\nu}^2/2M$ and $\lambda_{\mu\nu}^{(\gamma)} = \hbar^2\gamma_{\mu\nu}/2M$ are the coupling reorganization energies corresponding to the linear ($\alpha_{\mu\nu}$) and quadratic ($\gamma_{\mu\nu}$) attenuation parameters in the exponential dependence of the overlap integrals on the DAD, respectively, $\zeta = \coth\left[\beta\hbar\Omega/2\right]$, and $\beta = \left(k_{\text{B}}T\right)^{-1}$. The hydrogen vibrational wavefunctions used in the calculation of the overlap integrals and attenuation parameters were obtained as analytical solutions of the one-dimensional Schrödinger equation for a hydrogen (deuterium) moving in the

reactant and product diabatic potentials represented by Morse potentials for C–H (in the reactant) and O–H (in the product) bonds. The parameters of these Morse potentials are given in Ref. 7. The other parameters were determined utilizing available experimental data. The reaction free energies were calculated as $\Delta G_{\mu\nu} = \Delta G^{\circ} + \varepsilon_{\nu} - \varepsilon_{\mu}$, where ε_{μ} and ε_{ν} correspond to the proton vibrational state energy levels in the reactant and product diabatic potentials, respectively, and ΔG° was estimated to be –5.4 kcal/mol on the basis of experimental data.[8] The total reorganization energy, λ_{tot}, was chosen to be 13.4 kcal/mol for WT and 45.6 kcal/mol for DM-SLO to reproduce the temperature dependences of the absolute rate constant for WT SLO and DM SLO.[3] The effective mass *M* associated with the proton donor-acceptor mode was assumed to be 14 amu as determined in the molecular dynamics simulations of WT SLO.[8]

II. Figures S1-S7

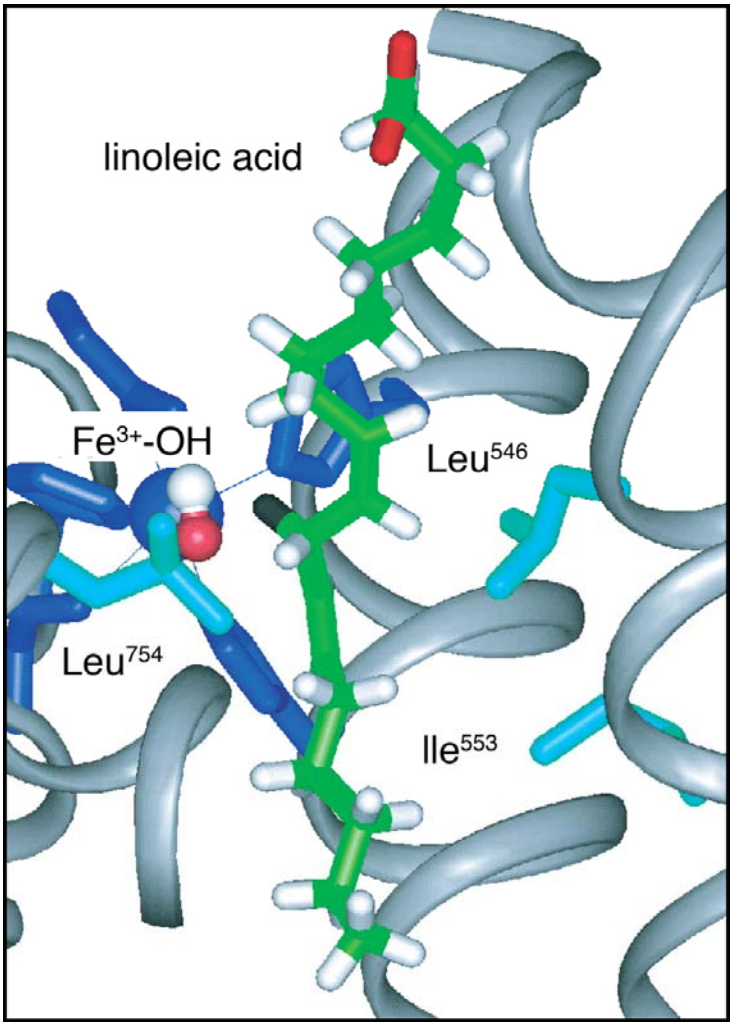

Figure S1: X-ray structure of the active site of SLO-1, with LA modeled into the active site. The side chains L546, L754, and I553 are shown in cyan. Figure taken from Ref. 1. Copyright (2008) National Academy of Sciences."

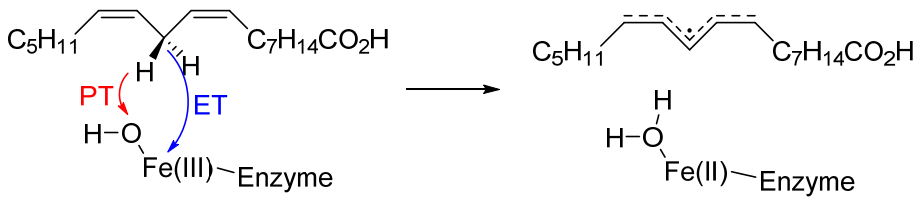

Figure S2: Schematic depiction of the PCET reaction catalyzed by SLO-1. The electron transfers from the π backbone of the linoleic acid to the non-heme iron Fe(III), and the proton transfers from C11 of the linoleic acid to the oxygen of the hydroxide bound to Fe(III) to generate water bound to Fe(II).

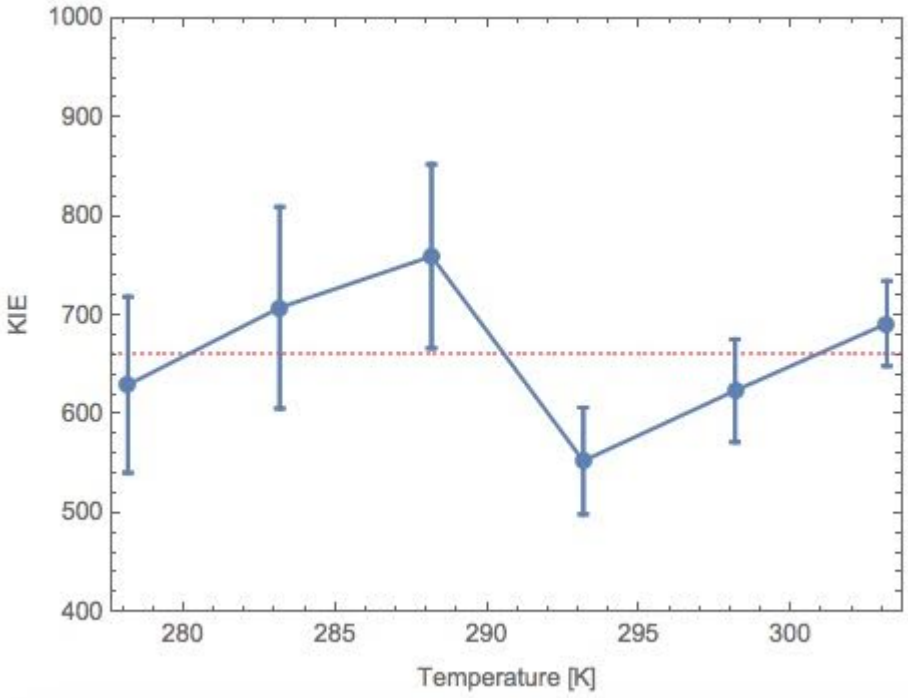

Figure S3: Temperature dependence of the experimentally measured KIE (with error bars) of the PCET reaction catalyzed by DM-SLO. The horizontal dotted line indicates the average KIE over the entire temperature range.

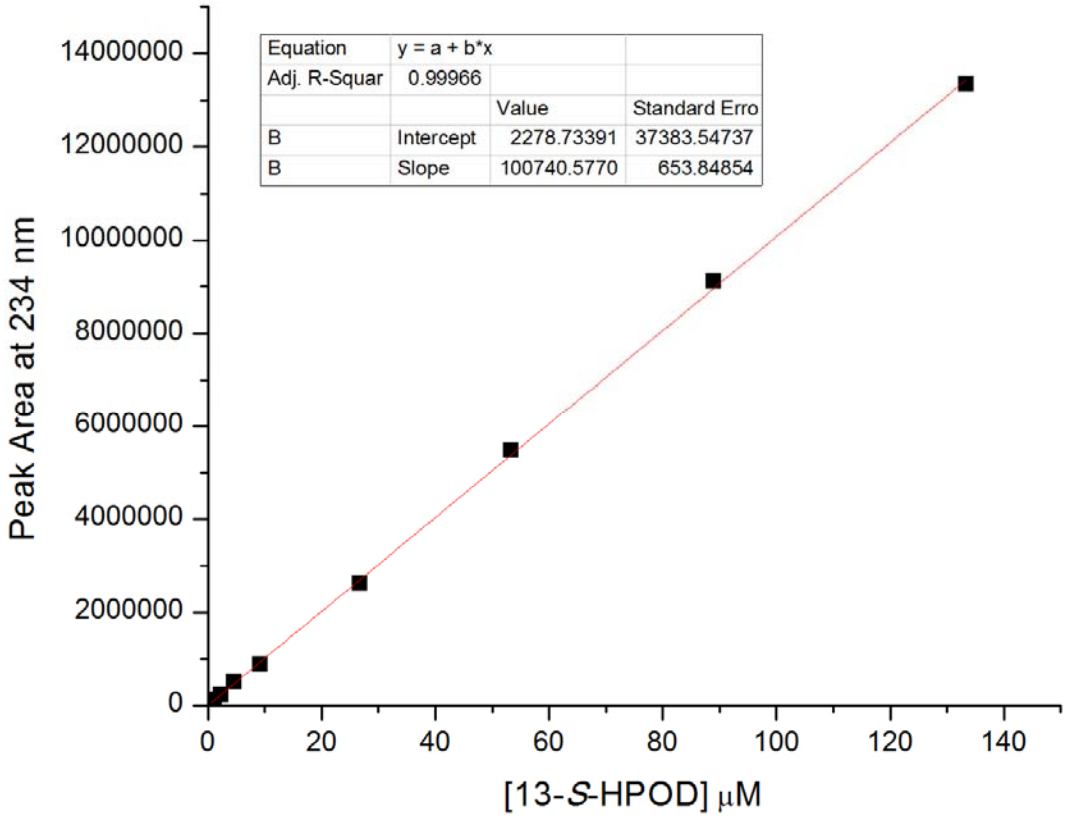

Figure S4: Calibration curve for the HPOD signal at 234 nm in the HPLC assay showing linearity of the signal with concentration of HPOD from 0–140 μM.

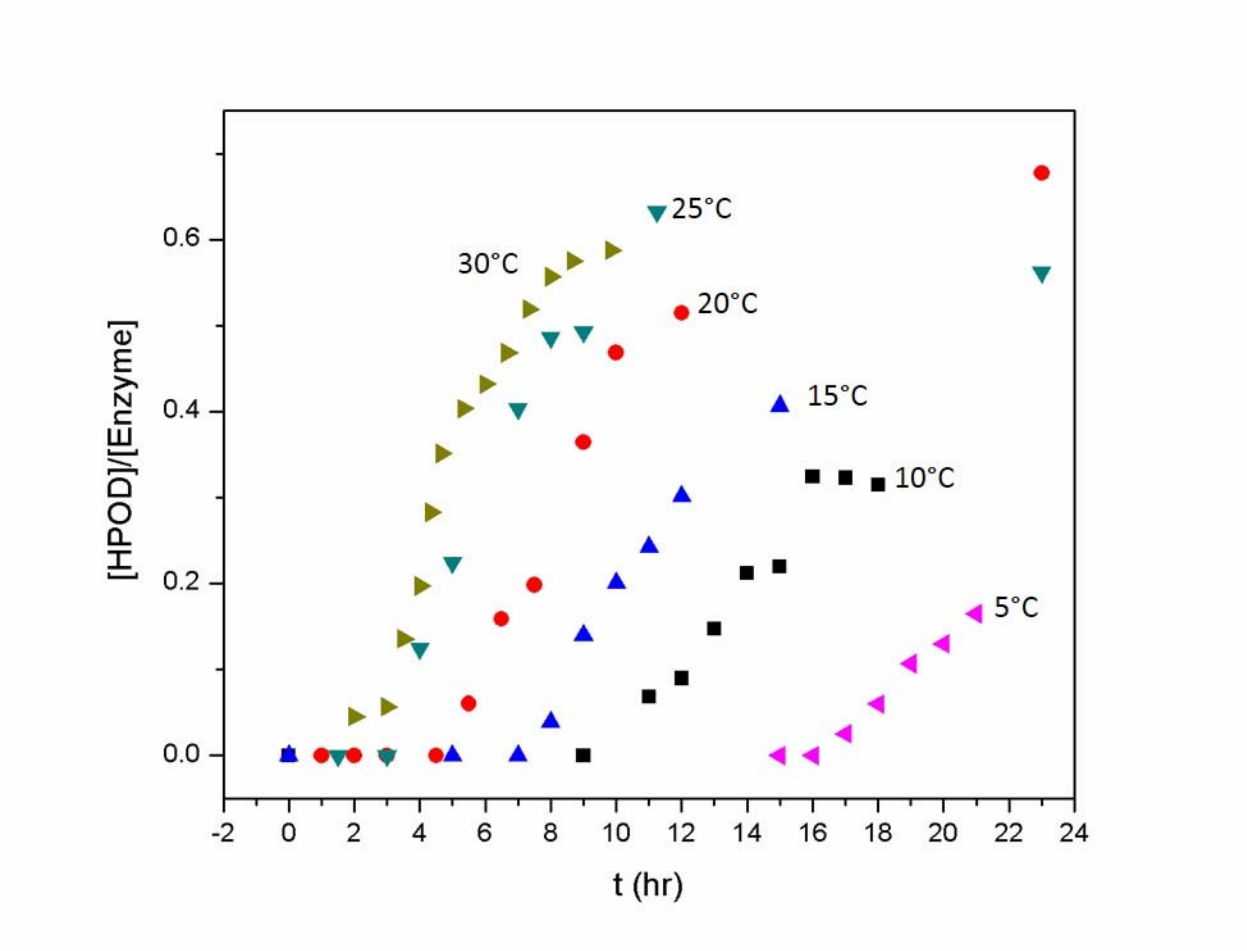

Figure S5: Time course of reaction of DM SLO (0.6 – 1.2 μM in the reaction mixer based on the temperature) with 35 μM d_2-LA in 0.1 M borate buffer (pH = 0.9). The points were obtained from the area of the product peak at 234 nm after correction by the standard curve and enzyme concentration.

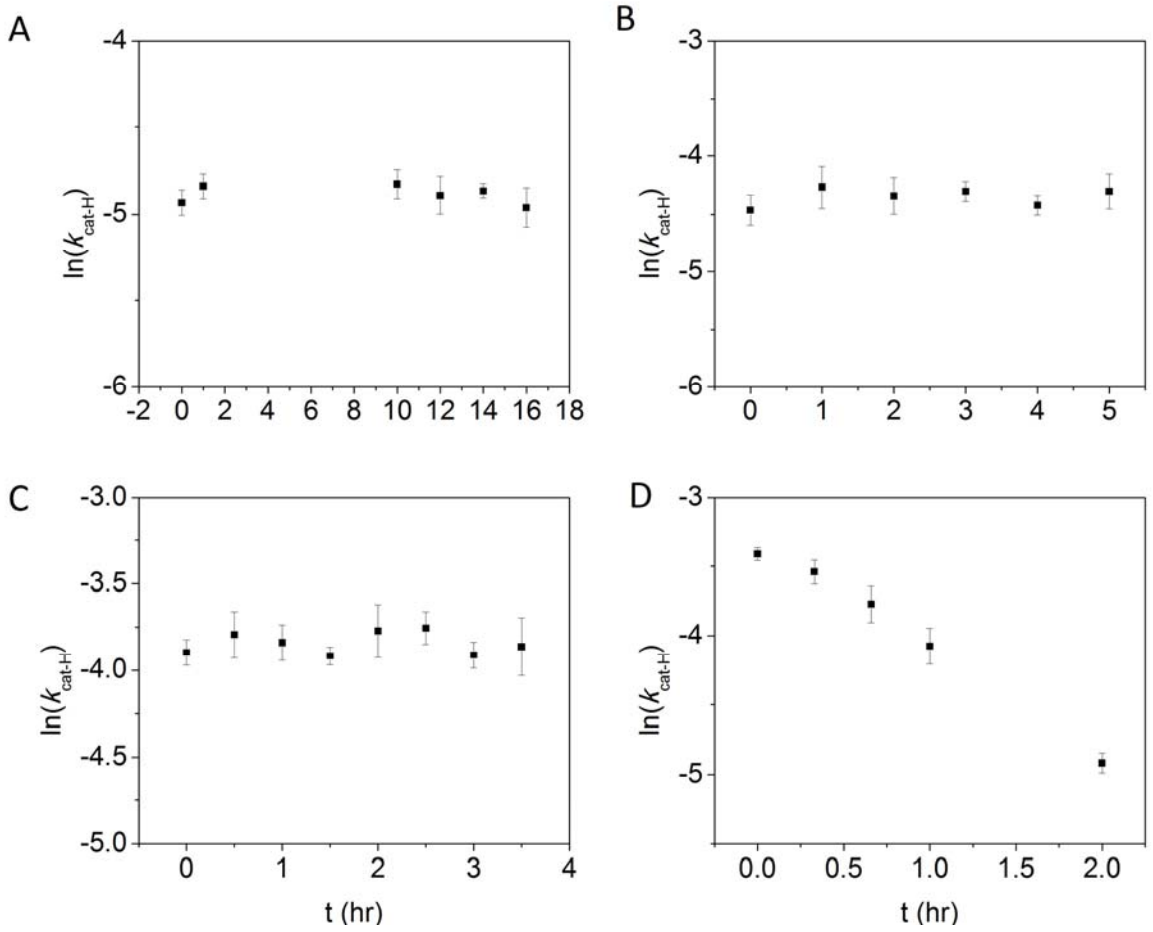

Figure S6: Stability of the DM SLO under conditions of the discontinuous HPLC assays in the presence of an equimolar amount of d_2-LA and enzyme (1.2 μM) at 5°C (A), 20°C (B), 30°C (C) and 35°C (D). At the indicated time points, the enzyme was diluted and assayed for the activity with the protio-LA substrate.

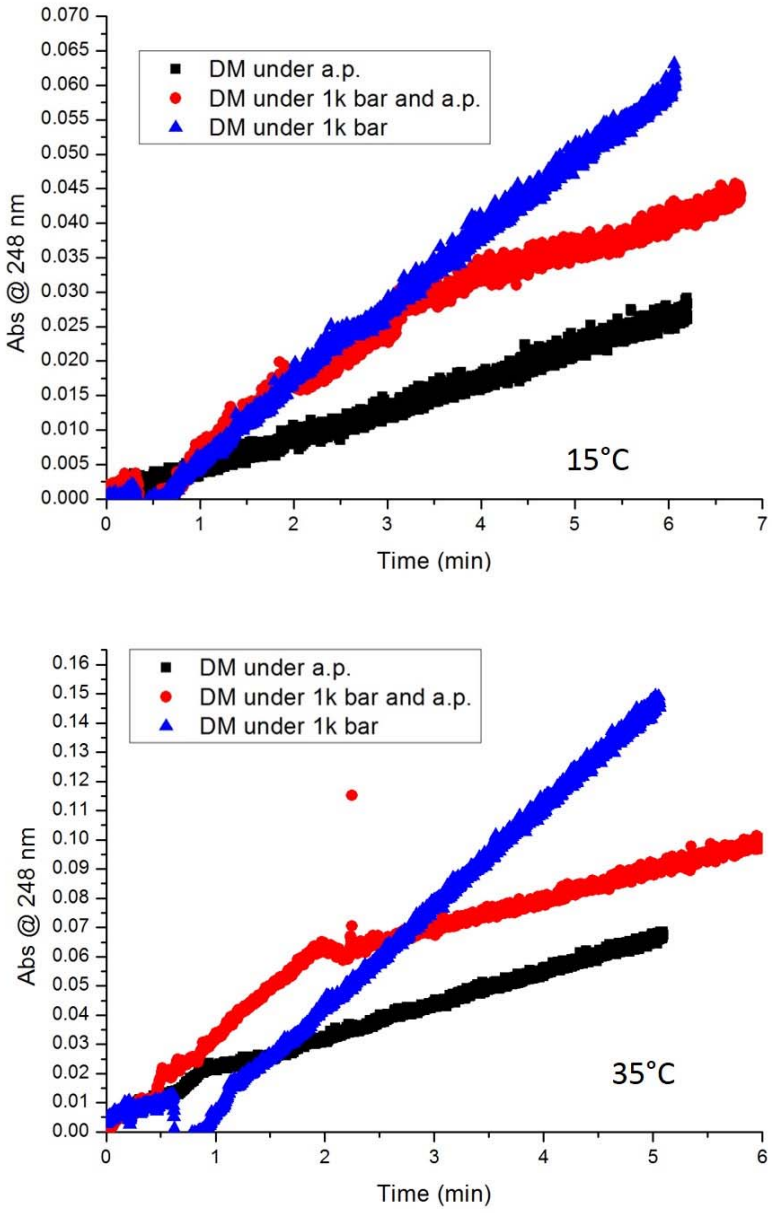

Figure S7: The DM-SLO stability under the "pressure-depressurize" assay at 15°C and 35°C. The DM SLO concentration was 800 μM. The concentration for H-LA was 100 μM for both cases.

III. Tables S1-S3

Table S1. The KIEs (at 30°C) and temperature dependencies of KIEs of WT SLO and active site variants.

Enzyme	$^{D}k_{cat}$	ΔE_a (kcal/mol) [a]	Ref
WT	81 (5)	0.9 (0.2)	4
L546A	93 (9)	1.9 (0.6)	4
L754A	112 (3)	2.0 (0.5)	4
I553A	93 (4)	4.0 (0.3)	4
I553V	82 (6)	2.6 (0.5)	1
I553G	178 (16)	5.3 (0.7)	1
I553L	81 (3)	3.4 (0.6)	1
L546A/I553A	128 (3)	2.8 (0.4)	9
L546A/L754A	692 (43)	0.3 (0.7)	Current study

[a] ΔE_a is the difference between the empirical activation energies for protium substrate and deuterium substrate (E_{aD}-E_{aH}), where E_{aH} and E_{aD} are obtained from the Arrhenius fitting of the corresponding rate constants at different temperatures.

Table S2. Kinetic parameters for L546A/754A at different temperatures and pressures.

T (K) / *P* (bar)	288	293	298	303	308
k_{cat-H} (10^{-2} s^{-1})					
1	1.17 (0.06)	2.23 (0.11)	2.71 (0.09)	3.39 (0.13)	4.30 (0.20)
344	2.29 (0.19)	2.84 (0.13)	3.54 (0.18)	4.49 (0.18)	5.51 (0.21)
688	3.03 (0.24)	3.69 (0.32)	4.71 (0.53)	5.69 (0.36)	7.20 (0.54)
1034	3.26 (0.22)	3.96 (0.25)	5.25 (0.31)	6.25 (0.29)	8.24 (0.48)

Table S3. Proton donor-acceptor equilibrium distance R_0, effective frequency Ω, and effective force constant $k_{eff} = M\Omega^2$, as well as dominant tunneling distances R_{dom} (H) and R_{dom} (D), determined for WT SLO and a series of I553 mutants by fitting the experimental KIE magnitudes and temperature dependencies using the analytical rate constant expression with quadratic terms.[a]

	R_0, Å	R_{dom} (H), Å	R_{dom} (D), Å	Ω, cm^{-1}	$k_{eff} = M\Omega^2$, (kcal/mol)$Å^{-2}$
			M = 100 amu		
WT	2.770	2.703	2.645	132.8	149.6
I553V	2.894	2.758	2.676	105.5	94.32
I553L	3.002	2.802	2.701	92.81	73.05
I553A	2.973	2.792	2.697	96.34	78.71
I553G	3.242	2.915	2.783	81.98	56.99
			M = 10 amu		
WT	2.881	2.750	2.669	368.2	114.9
I553V	2.997	2.799	2.699	316.3	84.85
I553L	3.104	2.820	2.700	266.4	60.19
I553A	3.075	2.831	2.720	295.1	73.86
I553G	3.351	2.958	2.810	257.5	56.25
			M = 14 amu		
WT	2.850	2.737	2.662	319.9	121.5
I553V	2.965	2.786	2.691	271.0	87.21
I553L	3.073	2.829	2.718	243.2	70.23
I553A	3.043	2.819	2.713	251.5	75.09
I553G	3.317	2.945	2.802	217.9	56.38

[a] The fitting to experimental data to obtain R_0 and Ω, as well as k_{eff}, for each mutant was performed using the analytical rate constant expression with quadratic terms, as given by Eq. (S1).[7] The dominant tunneling distances for H and D, R_{dom} (H) and R_{dom} (D), were determined subsequently using the thermally averaged expression in Eq. (2) of the main paper in conjunction with the probability distribution function $P(R)$ associated with a quantum harmonic oscillator. These dominant distances are defined to be the value of R at which the integrand in Eq. (2) is the largest value.

IV. References

1. Meyer, M. P.; Tomchick, D. R.; Klinman, J. P. *Proc. Natl. Acad. Sci. U. S. A.* **2007**, *105*, 1146-1151.

2. Sharma, S. C.; Klinman, J. P. *Biochemistry* **2015**, *54*, 5447-5456.

3. Hu, S.; Sharma, S. C.; Scouras, A. D.; Soudakov, A. V.; Carr, C. A. M.; Hammes-Schiffer, S.; Alber, T.; Klinman, J. P. *J. Am. Chem. Soc.* **2014**, *136*, 8157-8160.

4. Knapp, M. J.; Rickert, K.; Klinman, J. P. *J. Am. Chem. Soc.* **2002**, *124*, 3865-3874.

5. Hu, S.; Cattin-Ortolá, J.; Munos, J. W.; Klinman, J. P. *Angew. Chem. Int. Ed.* **2016**, *55*, 9631-9634.

6. Soudackov, A. V., Hammes-Schiffer, S. *J. Chem. Phys.* **2015**, *143*, 194101.

7. Soudackov, A. V., Hammes-Schiffer, S. *Farad. Discuss.* **2016**, *195*, 171-189.

8. Hatcher E.; Soudackov A. V.; Hammes-Schiffer, S. *J. Am. Chem. Soc.* **2007**, *129*, 187-196.

9. Sharma, S. C.; Klinman, J. P. *J. Am. Chem. Soc.* **2008**, *130*, 17632-17633.